Ecological Indicators 160 (2024) 111882

Contents lists available at ScienceDirect

Ecological Indicators

journal homepage: www.elsevier.com/locate/ecolind

One small step for a robot, one giant leap for habitat monitoring: A structural survey of EU forest habitats with Robotically-mounted Mobile Laser Scanning (RMLS)

Leopoldo de Simone [a,*], Emanuele Fanfarillo [a,b], Simona Maccherini [a,b], Tiberio Fiaschi [a], Giuseppe Alfonso [c], Franco Angelini [c], Manolo Garabini [c], Claudia Angiolini [a,b]

[a] Department of Life Sciences, University of Siena, Via Mattioli, 4, Siena 53100, Italy
[b] NBFC, National Biodiversity Future Center, Palermo 90133, Italy
[c] Centro di Ricerca "Enrico Piaggio", and Dipartimento di Ingegneria dell'Informazione, University of Pisa, Largo Lucio Lazzarino 1, Pisa 56122, Italy

ARTICLE INFO

Keywords:
3D point cloud
Automatic tree segmentation
Beech forest structure
Conservation status assessment
LiDAR
Quadrupedal robot locomotion

ABSTRACT

EU States are mandated by the 92/43/EEC Habitats Directive to generate recurring reports on the conservation status and functionality of habitats at the national level. This assessment is based on their floristic and, especially for forest habitats, structural characterization. Currently, habitat field monitoring efforts are carried out only by trained human operators. The H2020 Project "Natural Intelligence for Robotic Monitoring of Habitats – NI" aims to develop quadrupedal robots able to move autonomously in the unstructured environment of forest habitats. In this work, we tested the locomotion performance, efficiency and the accuracy of a robot performing structural habitat monitoring, comparing it with traditional field survey methods inside selected stands of *Luzulo-Fagetum* beech forests (9110 Annex I Habitat). We used a quadrupedal robot equipped with a Mobile Laser Scanning system (MLS), implementing for the first time a structural monitoring of EU forest habitats with a Robotically-mounted Mobile Laser Scanning (RMLS) platform. Two different scanning trajectories were used to automatically map individual tree locations and extract tree Diameter at Breast Height (DBH) from point clouds. Results were compared with field human measurements in terms of accuracy and efficiency of the survey. The robot was able to successfully execute both scanning trajectories, for which we obtained a tree detection rate of 100 %. Circular scanning trajectory performed better in terms of battery consumption, Root Mean Square Error (RMSE) of the extracted DBH (2.43 cm or 10.73 %) and prediction power ($R^2_{adj} = 0.72$, $p < 0.001$). The RMLS platform improved survey efficiency with 19.31 m^2/min or 1.77 trees/min in comparison with 3.45 m^2/min or 0.32 trees/min of traditional survey. Finally, a processing script was developed to allow the repeatability of RMLS surveys in similar habitat monitoring missions. In the future, a human-robotic monitoring framework might represent an accurate support for those repetitive and time-consuming activities in habitat monitoring, offering a valuable benefit for biodiversity conservation.

1. Introduction

Habitats are considered fundamental indicators of biodiversity and represent essential tools for nature conservation. Detecting their presence and assessing their Conservation Status (CS) is of vital importance for designing networks of protected areas, management planning, monitoring environmental impacts and setting targets for ecological restoration (Chytrý et al., 2020). In the European Union territory, the Directive 92/43/EEC of the European Council (hereafter "Habitats Directive") identifies habitats (as listed in Annex I) and species (as listed in Annex II, IV, and V) of Community interest, representing a cornerstone in terms of EU nature conservation policies (European Commission, 1992; Evans and Arvela, 2011). Moreover, the Habitats Directive states that CS and trends of species and habitats of Community interest should be assessed every six years for all EU Countries (Art. 11 and 17) to verify the effectiveness of conservation measures and the achievement of conservation targets. Habitat monitoring campaigns implemented to carry out such assessments require personnel with high levels of

* Corresponding author.
E-mail address: leopoldo.desimone@unisi.it (L. de Simone).

https://doi.org/10.1016/j.ecolind.2024.111882
Received 23 January 2024; Received in revised form 4 March 2024; Accepted 10 March 2024
Available online 18 March 2024
1470-160X/© 2024 The Author(s). Published by Elsevier Ltd. This is an open access article under the CC BY-NC-ND license (http://creativecommons.org/licenses/by-nc-nd/4.0/).

botanical expertise and the ability to move for long periods in unstructured environments, i.e., environments that present obstacles, uneven terrains, and hindrances. These requirements constitute the limiting factor of the EU habitat field monitoring efforts, because their implementation can only be carried out by highly specialised surveyors. This in turn implies elevated costs in terms of economic and human resources for the EU State members.

To solve this issue, the European Union project "Natural Intelligence for Robotic Monitoring of Habitats – NI " introduces an innovative concept to help human surveyors in performing terrestrial habitat monitoring. In Angelini et al. (2023a), we describe the idea of the NI project, which is to employ legged robotic systems to autonomously acquire relevant data for habitat monitoring. A legged robot enables to achieve higher traversability than wheeled systems and longer battery duration than traditional aerial systems. In fact, locomotion stands as an important issue for ground robots, which usually have difficulties in the movement over irregular and unstructured terrains (Angelini et al., 2023a, 2023b; Oliveira et al., 2021; Pollayil et al., 2023; Torres-Pardo et al., 2022). The ultimate goal of the NI project is to help human surveyors acquire useful data for habitat monitoring and the assessment of habitat CS.

Art. 1 of Habitats Directive defines the CS of a habitat as "favourable" if "specific structure and functions which are necessary for its long-term maintenance exist and are likely continue to exist for the foreseeable future". This is particularly important for forest habitats, whose structural characteristics are determinant to predict forest dynamics, interpret previous silviculture managements, define future stand-oriented management strategies, and interpret patterns of species richness and distribution (Angiolini et al., 2021; Barbati et al., 2014; Storch et al., 2018). The modifications of structural and compositional aspects of EU forest habitats for specific functions (Kuuluvainen, 2009; Lindenmayer et al., 2000; Raison et al., 2001) emphasises the importance of monitoring changes using accurate indicators (Evans and Arvela, 2011).

Tree Diameter at Breast Height (DBH), their number and spatial location are extensively used in local and national forest inventories to describe forest structural characteristics (Beers, 1962; Chang et al., 2015; Curtis and Marshall, 2005; Hyyppä and Inkinen, 1999; Köhl et al., 2006). DBH is important to calculate parameters like individual basal area, annual growth, height, and crown size (Köhl et al., 2006). Tree location data is ecologically significant for predicting growth, density, and species distribution patterns (Liang et al., 2018). These variables have been used also in habitat monitoring for evaluating the CS of forest habitats, as exemplified by studies such as those conducted by Alberdi et al. (2019), Corona et al. (2011), Chirici et al. (2012), and Kovač et al. (2014).

In the field, traditional surveys utilise callipers to directly measure the DBH and/or a diameter tape to measure the circumference of the trunk and extrapolate the tree DBH, whereas tree location data are predominantly obtained through close-range traversals employing a compass and a 100-metre tape measure (Köhl et al., 2006; West, 2015). Due to the time required for the repetitive task of measuring these parameters, traditional field surveys are usually spatially limited and labour intensive (Bauwens et al., 2016; Sun et al., 2018; Tremblay et al., 2020; Vítková et al., 2016). In recent years, other methods of collecting these structural data have been proposed, among which below-canopy photogrammetry (Krisanski et al., 2018) and the use of laser scanning technology (Light Detection and Ranging sensors, LiDAR; Bauwens et al., 2016). In particular, LiDAR sensors are widely applied in forest ecology under different survey approaches: Airborne Laser Scanning (ALS; Vauhkonen et al., 2014), Terrestrial Laser Scanning (TLS; de Conto et al., 2017; Liu et al., 2018; Maas et al., 2008), Mobile Laser Scanning (MLS; Čerňava et al., 2017; Chiappini et al., 2022; Dalla Corte et al., 2020), or a combination of them (Paris et al., 2015).

A top-to-bottom scanning direction and high elevation flights create limitations in direct DBH measurements from ALS surveys due to the derived scarce number of trunk points (Kankare et al., 2014). TLS surveys, preferred for direct DBH measurements, provide high-density point clouds but require multiple scanning stations to limit trunk occlusion, leading to lengthy surveys and substantial manpower needs (Bauwens et al., 2016; Gollob et al., 2020, 2023; Holopainen et al., 2013; Liu et al., 2018; Srinivasan et al., 2015; Wilkes et al., 2017). Recent exploration focuses on Unmanned Aerial Vehicles (UAV)-based MLS (ULS) surveys to extract, among other parameters, direct DBH measurements (Buchelt et al., 2024). However, challenges related to canopy occlusion persist (Brede et al., 2017, 2019; Dalla Corte et al., 2020; Schneider et al., 2019; Terryn et al., 2022; Vandendaele et al., 2021). Solutions to the canopy occlusion problems require specific acquisition planning, including high pulse repetition rates, multiple flight directions, and acquisition angles below 20° (Brede et al., 2022). Moreover, ULS have strict logistic requirements in terms of visual line of sight between the pilot and the aerial vehicle, which is challenging in forest environments (Sivanpillai et al., 2019). Terrestrial MLS methods overcome the canopy occlusion problem derived from the top-to-bottom scanning direction by using an under-canopy moving laser scanner (Cabo et al., 2018; Gollob et al., 2020, 2023; Mokroš et al., 2021). Terrestrial MLS are usually carried by operators with a backpack system or hand-held (Handheld Mobile Laser Scanning, HMLS; Wearable Laser Scanning, WLS; or Portable Laser Scanning, PLS) or are mounted on manned terrestrial vehicles. This way, the dynamic scanning derived by the terrestrial MLS systems significantly reduces times and costs of the survey.

Few studies used MLS sensors mounted on robotic platforms in semi-structured to unstructured forest environments (see Oliveira et al., 2021). Pierzchała et al. (2018) pioneered the use of a wheeled robot equipped with a LiDAR sensor and a microcontroller with an Inertial Measurement Unit (IMU) and GPS in a semi-structured flat forest. Employing a 3D graph-SLAM (Simultaneous Localization And Mapping) approach, they extracted DBH measurements and assessed their accuracies. For similar aims in various forest types, Tremblay et al. (2020) utilised a different teleoperated wheeled robot equipped with a LiDAR sensor and an IMU. Conversely, Chirici et al. (2023) employed for the first time a teleoperated legged robot with a LiDAR sensor for carrying out forest inventories. However, a resulting noisy point cloud produced DBH RMSE values not inferior to 39.6 % and permitted the identification of only a few trees with a DBH $<$20 cm. These studies, collectively, demonstrated the viability of robotic approaches for 3D mapping, tree localization, and DBH extraction during forest inventories along transects. However, these works focused on the implantation of new and more efficient practices for forest inventories and, hence, do not follow standardized protocols for meeting the monitoring requirements outlined in the Habitats Directive. These requirements, in the case of EU habitats, involve habitat-specific monitored surfaces of fixed size and shape, where both floristic and structural data are extracted (Angelini et al., 2016; Chytrý and Otýpková, 2003; Gigante et al., 2016). To the best of our knowledge, the use of easily deployable mobile quadrupedal robots equipped with a MLS represents a previously unexplored method to acquire structural data in EU Annex I forest habitat monitoring. These data are commonly plot-based rather than transect-based, because the structural monitoring constitutes a portion of the field monitoring effort for the surveyors, which as well includes floristic relevés. The latter consist in the recording of presence and cover abundance of each species growing in the plot (Ellwanger et al., 2018; Gigante et al., 2016).

In Angelini et al. (2023a), we describe the NI project idea of employing a quadrupedal robot to assist humans in habitat monitoring. Specifically, we use the ANYmal C robot (Hutter et al., 2017) for data gathering. In Angelini et al., (2023b), Angelini et al., (2023c), Angelini et al. (2024) and Pollayil et al. (2023), we provide examples of relevant data acquisition for habitat monitoring in four different habitats: grasslands, screes, dunes, and forests. In Kaur et al. (2023) and Manh et al. (2022), these data are used for species identification.

In this study, our main aim is to improve the human-based efforts in field monitoring EU forest habitats through the use of a robotic

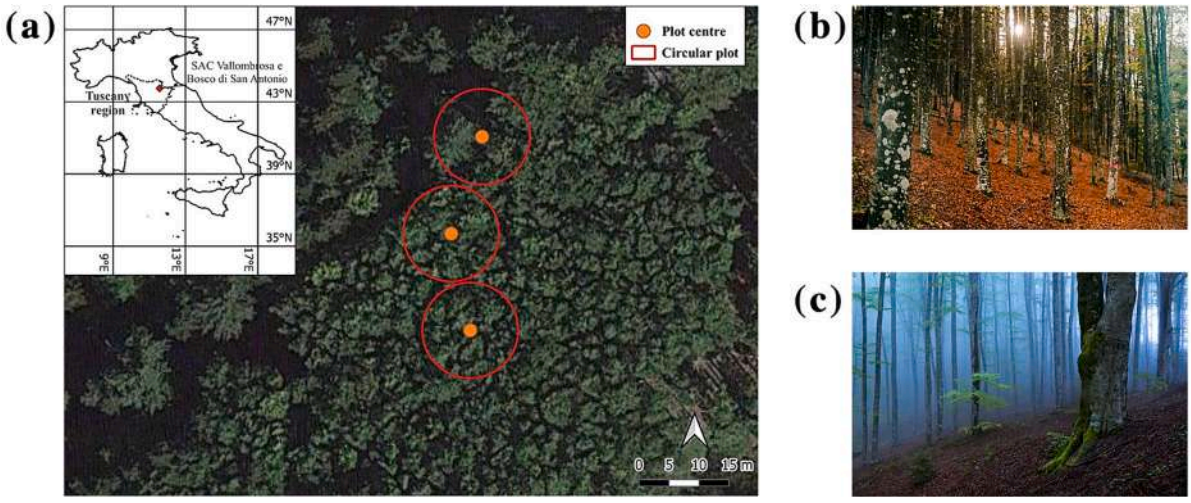

Fig. 1. Study area. a) Orthophoto of the study area with its geographic localization (top left) and the investigated circular plots. EPSG: 4326. b, c) Photos of EU Habitat 9110 in the study area.

workforce. Specifically, we explored the feasibility of a monitoring structural survey in forests through the employment of a quadrupedal robot equipped with a MLS. The objectives of this study are: i) assess the ability and performance of a legged robot in performing a EU forest structural habitat survey; ii) measure the accuracy of the extracted DBH using a Robotically-mounted Mobile Laser Scanning (hereafter "RMLS") survey compared to traditional field measurements; iii) evaluate the best scanning trajectory suitable for monitoring the forest structure using a RMLS survey; iv) estimate the efficiency of the RMLS survey in terms of monitoring time compared to traditional field surveys.

2. Materials and methods

2.1. Study area and traditional field survey

The study area is located within the Natura 2000 Network, in the Special Area of Conservation (SAC) "Vallombrosa e Bosco di San Antonio" (code IT5140012), in central Italy. The survey was carried out in a temperate forest of the EU habitat 9110 "*Luzulo-Fagetum* beech forests", an acidophilus beech forest type (Fig. 1). This habitat is characterised by a tree layer dominated by *Fagus sylvatica*, and a pauci-specific herbaceous layer composed of graminoid species such as *Luzula nivea* and *Avenella flexuosa*. Moreover, habitat 9110 has a relatively dense layer of leaf litter and decaying wood of different dimensions (Fig. 1b, c). The study area was selected for the ample presence of a mosaic among Habitat 9130 "*Asperulo-Fagetum* beech forests" and our investigated habitat, evaluated from the habitat map provided by the HaSCITu project (Habitat in the Sites of Conservation Interest in Tuscany; Tuscany Region, 2022) (Fig. 1b, c).

As for other EU forest habitats, the assessment of the CS of the habitat 9110 is performed with the measurement of parameters related to its structure and function, such as tree DBH, stem density, floristic data, and identification of typical and diagnostic species (Angelini et al., 2016; Gigante et al., 2016).

The structural survey was conducted in Autumn 2022. In accordance with similar works that monitored forest habitats listed in Annex I (Angiolini et al., 2021), we employed circular plots of circa 200 m^2 (radius = 8 m) inside an area characterised by the habitat 9110. Three plots were selected with similar stem densities, slopes, and the monospecific presence of mature individuals of *F. sylvatica* in the tree layer (Table 1).

Each plot centre coincided with the stem centre of a tree. The location of each plot centre was marked using a visible spray paint on the circumference of the central tree and its coordinates were recorded with a portable GPS device (Garmin Colorado 300). Georeferencing of each plot was executed with a minimum positional accuracy of 10 m (Garmin Colorado 300 owner manual). We used a measuring tape pivoting on the plot centre to delineate the circular plot boundaries (Baker and Pearson, 1981; Brown, 1974), outlining the surface where both the floristic and structural survey occurs and its centre, according to EU Habitat monitoring protocols (Angelini et al., 2016; Bunce et al., 2011).

It is worth mentioning that monitoring of EU forest habitats requires the georeferenced location of the plot rather than trees such as in forest inventories. However, since our aim was to compare traditional and RMLS surveys, a team of two botanists mapped within each plot the position and identity of each *F. sylvatica* tree. First, the location of each tree within the plot surface was mapped using a visible spray paint to colour a spot on the bark located at 1.2 m from the ground level. A unique identification number (assigned ID), in addition to the bearing and distance from the plot centre were subsequently measured for each tree (Vastaranta et al., 2009). We used a laser distance metre (Bosch GLM 50–22 professional) to measure the distance from the plot centre to the stem of each tree and a field compass to measure the bearing. Then, for each mapped tree within the plot, we measured the DBH using traditional field methods. Tree DBH was measured at a height of 1.20 m above ground in the uphill direction using a calliper (Köhl et al., 2006).

Table 1
Plot location, slope, number of trees encountered in the field and DBH_R values collected in the traditional field survey.

Plot	Coordinates (EPSG:4326)	Slope [deg °]	Number of trees	DBH_R range [cm]	Mean DBH_R (σ) [cm]	Stem density [trees/m^2]
1	43.745017 N 11.567416 E	17	19	16–32.5	23.47 (4.59)	0.1
2	43.745161 N 11.567486 E	18	19	14.5–28.5	21.87 (4.39)	0.1
3	43.744871 N 11.567449 E	16	17	18.5–29.5	22.56 (3.08)	0.09
Overall			55	14.5–32.5	22.64 (4.16)	0.09

To limit the effect of elliptical stems on DBH measurements, for each tree we recorded two calliper readings at right angles of the DBH and calculated the arithmetic mean to obtain the reference DBH value (DBH_R; Moran and Williams, 2002). To standardise the measurement of DBH among plots, readings were performed along the North-South and East-West axes.

2.2. Robotically-mounted MLS survey

As described in the previous section, EU habitat 9110 is typical of mountainous regions, and can occur on steep slopes. Moreover, the forest floor is characterised by a dense litter layer, which includes leaves, twigs and fallen branches, in addition to rocks and exposed tree roots. All these elements represent potential obstacles for ground robot locomotion, especially in the case of traditional wheeled systems. Legged robots can overcome this issue thanks to their greater ability to cope with irregular terrains (Angelini et al., 2023a; Torres-Pardo et al., 2022).

Fig. 2 shows the quadrupedal robot employed in this study, i.e., ANYmal C (Hutter et al., 2017). This robot is 0.6 m tall, has a body size of 1.05 m by 0.52 m, and weighs 50 kg. Each of its four legs presents three joints to enable hip abduction/adduction, hip flexion/extension, and knee flexion/extension. ANYmal C is equipped with a battery composed of lithium-ion based cells, whose energy is 932.4 Wh. As reported on the official specification, this robot can operate for 2–4 h on a single charge (Anybotics, 2022). Furthermore, according to official specification (Anybotics, 2022), ANYmal C can be operated in a temperature range of 0–40 °C, even in harsh environment. Indeed, the robot ingress protection is ruggedized, and water and dust-proof according to IP67.

The self-awareness of ANYmal C is achieved through a combination of sensors, including an IMU and joint encoders. The IMU is composed of an accelerometer and a gyrometer to measure body accelerations and angular rates, while the encoders measure the position of the leg joints. Joint actuators can also give information about joint torque, which is then used for estimating which foot is in contact with the ground. Information collected by these sensors are then used by a sensor fusion algorithm to estimate the robot state, consisting of its position, orientation, velocity, and leg orientation w.r.t. the robot body.

The ability of the robot to perceive and understand its surroundings comes from a wide range of sensors, i.e., six cameras and a LiDAR sensor. The six cameras are: two wide-angle cameras located respectively on the front and back, and four depth cameras (one on each side) with a mounting angle with respect to horizon equal to 30° downwards. The LiDAR sensor is placed on top of the robot in the rear part (Fig. 2). The main sensors used to reconstruct the surrounding environment are the four depth cameras and the LiDAR sensor. Depth cameras, also known as RGB-D cameras, are able to provide range information in addition to colour image data. This is achieved by projecting a randomised pattern of light onto a scene, and then measuring the distortion of the pattern to calculate the distance to objects. The RGB-D cameras mounted on ANYmal C are Intel RealSense D435, whose specifications are reported in Table 2. The LiDAR sensor generates a three-dimensional representation of the environment by emitting laser pulses to then measure the time taken for the reflected light to return. The LiDAR sensor mounted on ANYmal C is a Velodyne VLP-16 puck LITE, whose specifications are reported in Table 2. Given these specifications, these types of range sensors return different point clouds with specific fields of views and frequency. An onboard sensor fusion algorithm merges these data sources to create a richer and more complete point cloud. This is achieved by selecting high information content, removing unnecessary points (e.g., robot body or legs), and transforming data to a common reference frame also thanks to the robot state information.

ANYmal C has three onboard computers to enable locomotion and

Table 2
Specifications of the RGB-D cameras and LiDAR.

RGB-D cameras	
Model	Intel Realsense D435
Mounting angle with respect to horizon	30° downwards
Depth Camera Field of View (DxHxV)	95°×87°×58°
Depth Camera Shutter Type	Global
Max. Depth Image Resolution	1280×720 pixels
Max. Depth Image Framerate (at full resolution)	30 frames per second
Depth Range	0.1 to 10 *m*
Color Camera Field of View (DxHxV)	77°×69.4°×42.5°
Color Camera Shutter Type	Rolling
Max. Color Image Resolution	1920×1080 pixels
Max. Color Image Frame rate (at full resolution)	30 frames per second
LiDAR sensor	
Model	Velodyne VLP16 Puck LITE
Number of Channels	16
Accuracy (typical)	3 cm
Measurement Range	0 to 100 *m*
Horizontal Field of View	360°
Horizontal Angular Resolution	0.1° to 0.4°
Vertical Field of View	−15° to 15° (30°)
Vertical Angular Resolution	2.0°
Rotation Rate	5 Hz to 20 Hz

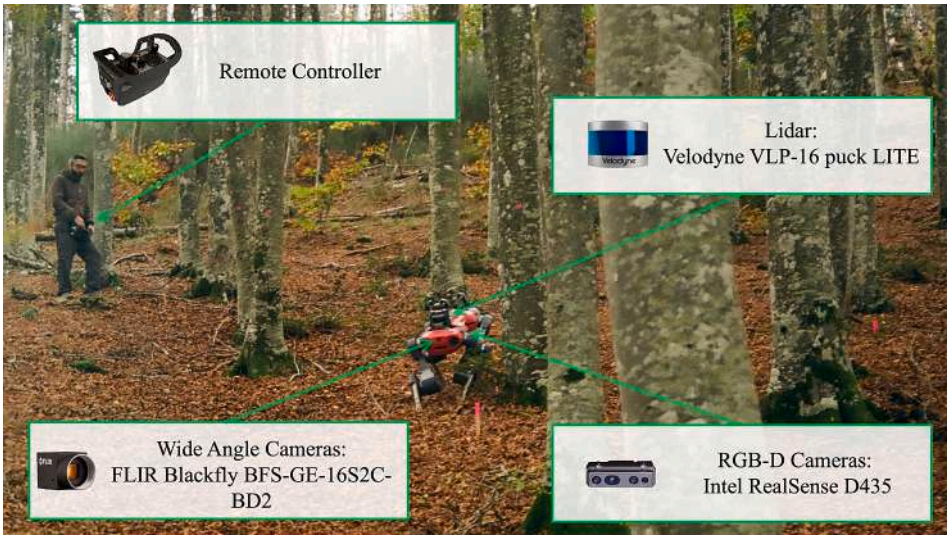

Fig. 2. ANYmal C robot surveying Habitat 9110.

task execution. Additionally, wireless communication can be set between the robot and the computer used by a human operator to enable real-time visualisation of the robot status and exteroception information, e.g., a live video stream of the robot cameras or SLAM output. Additionally, two operating modes can be used: autonomous and teleoperated. In the autonomous mode, the robot executes a pre-planned mission composed of a set of waypoints without the intervention of the human operator. Conversely, in teleoperated mode, the robot motion is controlled by a human operator. This is achieved by providing velocity commands to the robot through a remote controller, which is directly connected to the robot through a wireless communication network. In this study, the robot is used in teleoperated mode.

The robot locomotion is enabled by the onboard control algorithm. This is trained using a reinforcement learning-based method (Lee et al., 2020). In simulations, the algorithm learns a policy for controlling the robot by exploiting information about the robot's contact with the ground, the terrain profile, friction, and disturbances. Then, a student policy is trained to imitate the learned policy. The student policy only has access to the robot's command vector and the history of its joint and IMU measurements. The result is a controller that outputs desired joint positions, allowing the robot to robustly navigate challenging terrains at a maximum speed of 1 m/s.

Shortly after the completion of the traditional survey, the same day a team of two roboticists operated the robot for RMLS-based 3D point cloud collection within the same plot surfaces. The robot was transported to the study area using a van, which was parked on the roadside. Here, the robot was unloaded, placed on the ground, and turned on. At this point, one of the roboticists used the robot remote controller to teleoperate the robot toward the plot surfaces, which were identified using the previously recorded GPS coordinates of each plot centre. The distance between the parked van and the plot centres was approximately 100 m. Once arrived in the 10 m radius value of unknown around the true position of the plot centre, the roboticists used the visible spray paint on the central tree to place the robot in the plot centre. At this point, the other roboticists used a laptop to set a local wireless connection to the robot, then, using the ANYmal research Graphic User Interface, the MLS was initialised without the need of any dataset. This procedure requires less than one minute. Then, the RMLS survey started teleoperating at a walking speed pace. Thanks to the laptop-robot connection, the output of the SLAM can be visualized online on the laptop. This enables the roboticist to have a rough estimation of the position of the robot, w.r.t. the plot area to perform the structural survey without the need of physically marking the plot actual boundaries. Indeed, given the range of the LiDAR sensor (Tab. 2), and the information acquired by it, the actual plot area can be clipped a-posteriori from a larger scanned surface directly using the measured point cloud (Figs. 3 and 4).

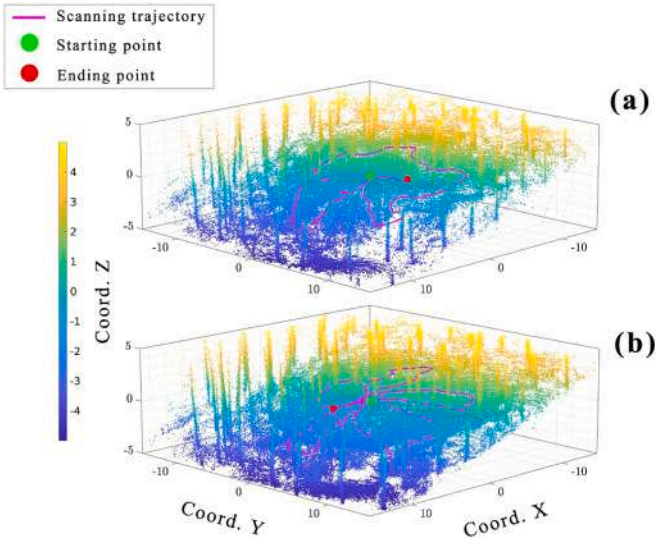

Fig. 3. Scanning trajectories of the RMLS survey. Only a 20×20×10 m portion of the original point cloud centred in the plot position is shown in figure. Starting and ending points and the different scanning trajectories are shown. Colour gradient denotes the values of coordinate Z. (a) scanning trajectory A; (b) scanning trajectory B.

ANYmal C surveyed each plot twice, using two different scanning trajectories. Scanning trajectories were repeated similarly in each plot and were designed to: i) acquire a complete coverage of the survey area; ii) avoid stem occlusion and blind spots; and iii) reduce the drift error of the SLAM algorithm. The first scanning trajectory (scan A) was approximately circular, following the outer perimeter of the plot. The second scanning trajectory (scan B) followed a star-shaped trajectory adapted from Bauwens et al. (2016) and Gollob et al., (2020; Fig. 3). The point cloud data derived from each scan were registered in real time, allowing an instant visualisation of the survey data. Such real time feedback enabled the roboticist team to better perform data acquisition and avoid possible stem occlusions during the survey.

The resulting point clouds from the RMLS surveys were saved in .ply format and used a local coordinate system with the centre coinciding with the plot centre.

2.3. Point cloud processing and DBH extraction

Point cloud processing was performed using a PC with an AMD Ryzen 7 3700x 8-Core CPU, a DDR4 32 GB RAM and a NVIDIA GeForce GTX 1050 Ti 4 GB graphic card. The point cloud data processing workflow is described in Fig. 4.

After the completion of field data acquisition, each couple of point clouds pertaining to the same plot (scan A and scan B) were imported in the software CloudCompare (2023) for registration. To register scan A and scan B of each plot, we implemented a two-step process. First, we roughly registered the two scans using the tree location map and the assigned tree IDs. Then, we refined the alignment using the Iterative Closest Point (ICP) algorithm (Zhang, 1994). In this step, we used a threshold error (RMS) difference between iterations with a value of $1e^{-8}$.

After the registration, each couple of registered point clouds of the same plot was filtered to select only points belonging to the corresponding plot space. For this purpose, all points positioned outside the inner volume of a cylinder with a radius of 8 m centred in the plot were deleted.

After this step, we calculated in CloudCompare the point verticality using a local neighbourhood radius of 0.5 m. Verticality is a geometric feature based on the eigenvector of the structure tensor (see Hackel et al., 2016) and is used in this work to better differentiate ground points.

Each point cloud was then exported in the format .las. All further analyses were performed using the R statistical software (R core team, 2022), importing each point cloud using the function *readLAS* of the package lidR (Roussel et al., 2020). DBH extraction was performed on each point cloud separately following a series of preparing steps. Though, all point clouds underwent the same steps and equal parameters were used along the entire workflow.

First, point clouds were filtered from outliers to reduce noise points using the Statistical Outlier Removal algorithm (Rusu and Cousins, 2011). For this purpose, we used the function *classify_noise* in the package lidR. The algorithm computed the mean distance of each point to all its k-nearest neighbours and used it m-times as a threshold to segment outliers. We used k = 6 and m = 1 as parameters for this step (Kükenbrink et al., 2022).

Next, we classified ground points in the denoised point clouds to normalise tree heights using a Cloth Simulation Filter (CSF) using the function *classify_ground* in the package lidR (see Zhang et al., 2016). After several iterations, we used a class threshold of 0.5 m and a cloth

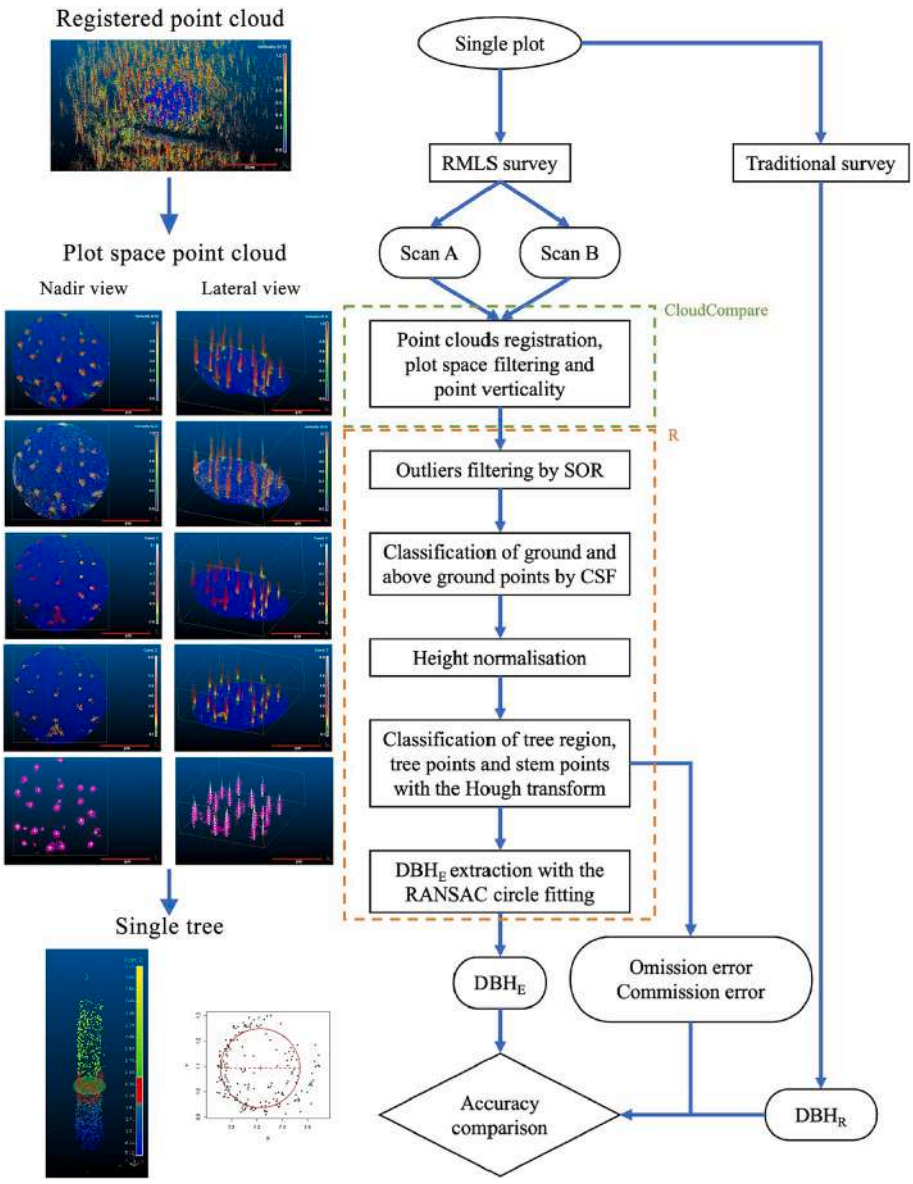

Fig. 4. Research workflow of point cloud processing to extract and compare data from the 3D point cloud. SOR = Statistical Outlier Removal; CSF = Cloth Simulation Filter; RANSAC = Random Sample And Consensus.

resolution of 0.1 m for this step. All other parameters were left as default. However, visual inspections of point clouds showed that some points pertaining to the tree trunks were erroneously classified as ground points. We then filtered the tree trunk points which were erroneously classified as ground points and subsequently reclassified them as above ground points by using their verticality value (a value which ranges from 0 to 1). For this purpose, we included all points with a verticality value higher than or equal to 0.5 (threshold based on visual inspection).

After ground classification, point clouds were height normalised to automatically extract their DBH (hereafter DBH_E [cm]). This step was necessary for DBH_E extraction to obtain measurements taken at the same height relative to the ground for each tree. This process involved the interpolation of the elevation for each individual point in relation to points classified as ground, as opposed to relying on elevations at specific predefined locations using a Digital Terrain Model. To normalise point clouds, we used the function *normalize_height* in the package lidR using a spatial interpolation algorithm that employs a k-nearest neighbour approach with inverse-distance weighting for interpolation. For this step, we left all parameters as default.

Height normalised point clouds were processed to extract DBH_E automatically using the package TreeLS (de Conto et al., 2017). First, normalised point clouds underwent the removal of points below 0.1 m and above 6 m. This step had the purpose to streamline the processing and emphasise the representation of stem segments for their DBH_E extraction, significantly reducing processing time and potential outliers. Then, we used the function *treeMap* to locate tree occurrence regions employing a Hough transform circle search algorithm. The Hough transform is a robust algorithm valued for its ability to handle noisy data effectively (Chiappini et al., 2022; de Conto et al., 2017; Kuželka et al., 2022; Simonse et al., 2003). It is used for identifying basic shapes (Illingworth and Kittler, 1987) such as circles, whose search stands out as a widely adopted method for detecting tree stems. For this step, we used a minimal point density of <0.0001 and a height threshold of points higher than 0.5 m to exclude understorey vegetation and lower tree trunks. All other parameters were maintained as default. Furtherly, the function *treePoints* was employed to classify and assign a unique tree identification number (extracted tree ID) to those points located within a circle of 1 m radius of each tree region. Tree points were subsequently filtered from outliers and classified as stem points using the function

stemPoints. For this purpose, we applied again the Hough transform circle search algorithm to further filter noise points. In this work, we used the following parameters to carry out stem points classification: i) maximum stem diameter of 35 cm (a value higher than the largest DBH_R measurement in the dataset) to filter out larger clusters of points that might be associated with lower tree branches and leaves; ii) a minimum point density within a pixel evaluated on the Hough transform of 0.2 points/m^2 to allow only dense clusters of points to undergo circle search; iii) a minimum number of three circle intersections over a pixel to assign it as a circle centre candidate (for details, see de Conto et al., 2017). All other parameters were maintained as default.

Finally, tree position and their DBH_E were automatically extracted from point clouds that underwent stem point classification using the function *tlsInventory* with the RANdom Sample And Consensus (RANSAC) circle fitting method. For this process, we executed the function by selecting a vertical segment of 0.4 m of points classified as a stem that is centred at a height of 1.20 m from ground level, whereas all other parameters were maintained as default. The location of detected trees was manually searched for a correspondence with the location of trees encountered in the field. Using field-acquired data on bearing and distance from the plot centre of each tree, a detected tree was deemed a correspondence if it was situated within a radius of 2 m of the tree encountered in the field (adapted from Kükenbrink et al., 2022). Detected trees that were situated at the borders of the plot region were discarded from the analysis. The complete point cloud dataset and the processing script are available in Appendix (supplementary material 1-7).

2.4. Comparison evaluation

To analyse the performance of the robot, we observed whether it could walk on the inclined terrain within the study area. From the point of view of the energetic cost of the RMLS survey, we measured the total travelled distance and the total battery consumption for each scanning trajectory.

The evaluation of the accuracy and the efficiency of the RMLS survey was performed using an overall dataset, i.e. merging the partial results derived from single plots that were scanned using the same trajectory.

Accuracy of tree detection was evaluated using: i) Tree Detection Rate (TDR [%], Eq. (1); ii) omission error or the number of not detected trees; and iii) commission error or the number of falsely detected trees.

$$TDR\ [\%] = \frac{\eta_{match}}{\eta_{ref}} \times 100 \tag{1}$$

where η_{match} is the number of trees that were correctly matched with trees encountered in the field, and η_{ref} is the total number of trees encountered in the field.

The accuracy of the automatically extracted DBH_E measurements was evaluated by a linear regression to assess the degree of correspondence of DBH_E to the reference measurements. We also calculated the absolute and relative Root Mean Square Error (RMSE [cm], Eq. (2); and RMSE [%], Eq. (3)), which is the square root of the mean quadratic deviation between DBH_E and DBR_R. To calculate RMSE [%], we used the mean DBH_R (Eq. (4)).

$$RMSE\ [cm] = \sqrt{\frac{1}{\eta_{match}} \sum_{i=1}^{\eta_{match}} (DBH_E - DBH_R)^2} \tag{2}$$

$$RMSE\ [\%] = \frac{RMSE\ [cm]}{\overline{DBH_R}} \times 100 \tag{3}$$

$$\overline{DBH_R}\ [cm] = \frac{1}{\eta_{match}} \sum_{i=1}^{\eta_{match}} DBH_R \tag{4}$$

Moreover, we calculated the absolute and relative bias (bias [cm], Eq. (5); and bias [%], Eq. (6)), which is the mean deviation between DBH_E and DBR_R.

$$bias\ [cm] = \frac{1}{\eta_{match}} \sum_{i=1}^{\eta_{match}} (DBH_E - DBH_R) \tag{5}$$

$$bias\ [\%] = \frac{bias\ [cm]}{\overline{DBH_R}} \times 100 \tag{6}$$

To assess the efficiency of RMLS survey, we recorded and compared survey times used to complete the traditional and the RMLS monitoring mission. The overall survey time using traditional methods was calculated as the sum of the time used to: i) place the plot boundaries; ii) map the position of each tree in the plots and assign its reference number; and iii) measure the DBH_R. The overall survey time using the RMLS survey was calculated as the sum of the time used to: i) scan and record the point clouds; and ii) process the 200 m^2 point clouds to extract DBH_E values. We measured survey time in field operations with a chronometer and in point cloud processing with the PC internal clock. Survey efficiency was calculated using two indices, accounting for both survey methods and for each scanning trajectory of the RMLS survey: surface monitored [m^2/min] (Eq. (7), Chen et al., 2019; Ko et al., 2021) and trees monitored [trees/min] (Eq. (8).

$$surface\ monitored\ \left[\frac{m^2}{min}\right] = \frac{overall\ plot\ surface\ [m^2]}{overall\ survey\ time\ [min:sec] \times number\ of\ surveyors} \tag{7}$$

$$trees\ monitored\ \left[\frac{trees}{min}\right] = stem\ density\ \left[\frac{trees}{m^2}\right] \times surface\ monitored\ \left[\frac{m^2}{min}\right] \tag{8}$$

The latter index was created to enable future comparisons of this methodology with forest habitats that have different stem densities.

3. Results

In all plots and scanning trajectories, the robot was able to successfully walk on the inclined terrain of habitat 9110 despite the presence of leaves and other ground obstacles such as fallen branches, rocks, and roots. This is mainly achieved thanks to the performance and robustness of the employed reinforcement learning based controller (Lee et al., 2020). Fig. 5 shows a sequence of images where the robot is performing a scanning. A video recording of ANYmal C performing the RMLS survey is available in Appendix (supplementary material 8).

Results on the robot travelled distance for each scanning trajectory and its related energetic cost are reported in Table 3.

A total of 55 trees of *F. sylvatica* were found in our survey, with an almost similar number of trees among plots (Table 1). Table 4 shows the accuracy comparison among scanning trajectories.

No omission errors were detected both in scanning trajectory A and B, hence all trees encountered in the field were detected in the corresponding point clouds, achieving a TDR = 100 %. Conversely, falsely detected trees were more frequent in Scan A (7) than in Scan B (1). In scan A, the highest number of falsely detected trees was found in plot 1 [5], whereas the sole falsely detected tree of scan B was found in plot 2.

Scan A produced better results than Scan B in terms of RMSE: 2.43 cm or 10.73 % and 3.25 cm or 14.34 %, respectively. By contrast, bias was lower in scan B (−0.2 cm or −0.88 %) compared to scan A (0.44 cm or 1.96 %).

Fig. 6 shows how the two scanning trajectories used in the study lead to different performances of the DBH_E compared to DBH_R. Linear regression of DBH_E in scan A shows a higher correspondence to the reference measurements than in scan B ($R^2_{adj} = 0.72$, $P < 0.001$ and $R^2_{adj} = 0.52$, $P < 0.001$, respectively).

Table 5 compares the efficiency of the traditional and RMLS surveys. It resulted that using the RMLS survey, a single surveyor can structurally

Fig. 5. Photo-sequence of the ANYmal C robot performing Scan B for Plot 3.

Table 3
Comparison of travelled distance and battery consumption for the two scanning trajectories.

Scanning trajectory	Travelled distance [m]	Battery consumption [%]
Scan A	178	16
Scan B	206	26

monitor 19.31 m^2/min of habitat 9110 or 1.77 trees/min using a circular scanning trajectory (scan A) and 13.94 m^2/min or 1.28 trees/min using a star-shaped trajectory (scan B). In comparison, a surveyor that uses the traditional survey method can structurally monitor 3.45 m^2/min or 0.32 trees/min.

4. Discussion

A significant amount of time in the activity of EU habitat monitoring can be usually accounted for gathering structural data, which are a fundamental indicator of the dynamic differences and conservation status within forest habitat patches (Angelini et al., 2016, Angiolini et al., 2021). Our results proved for the first time that the use of a robotical assistance in performing accurate, time efficient EU forest habitat monitoring of structural data, such as habitat 9110 and similar forests, is achievable in the present time using a RMLS survey. Moreover, employing a legged robot with this RMLS-based monitoring protocol can enhance the efficiency of structural habitat monitoring by nearly sixfold using a circular trajectory in a forest habitat with a stem density of 0.1 stems/m^2.

Our quadrupedal robot demonstrated to be able to walk in unstructured environments despite the presence of ground obstacles and non-negligible terrain inclination. This condition was considered challenging in similar studies (Pierzchała et al., 2018; Tremblay et al., 2020). The motion controller running on ANYmal C (Lee et al., 2020) enables it to blindly walk over challenging terrains and to autonomously cope with ground obstacles like rocks, roots, and slippery grounds. Obstacles of size 10–15 cm are thus not avoided by the tele-operator and left to-be-dealt with to the robot itself. Larger obstacles like trees or boulders are instead avoided by slightly varying the location trajectory steering the robot. This overall behavior allows us to prevent major incidents like collisions or falls. Indeed, at the moment, the employed robot is able to cope with some external disturbances, but it is not able to autonomously recover from falls. However, in the state of the art there are algorithms (Lee et al., 2019; Yang et al., 2023) that enable this feature, and future version of ANYmal software will include autonomous fall recovery. From the efficiency point of view, scan B resulted in larger total travelled distance and total battery consumption and longer duration. Despite the fact that the percentage of increase of travelled distance between scan A and scan B was only ~ 16 %, the percentage of increase in battery consumption was more than 60 % (62.5 %). This result highlights that scanning trajectories requiring longer mission duration over an uneven terrain (such as that of our study area) lead a quadrupedal robot to sustain larger cumulative elevation gains. Then, following a more complex star-shaped trajectory such as that of scan B, required a larger energy consumption. Conversely, a simpler circular trajectory (scan A) resulted in a smoother and milder terrain inclination variation and less energy consumption. Hence, by using this scanning trajectory in similar environments, future RMLS surveys for structural habitat monitoring will be able to carry out the measurement of approximately eighteen 200 m^2 circular plots per single battery charge.

Both scanning trajectories produced a complete 100 % TDR in beech forests of EU habitat 9110 and, thus, represent both valid acquisition patterns to obtain a complete representation of the mapping area. In fact, MLS-derived point clouds have generally high TDR, with values ranging between 57 and 100 % (Balenović et al., 2021; Gollob et al., 2020; Kuželka et al., 2022). In general, MLS-derived point cloud occlusions are lower compared to above canopy point cloud acquisitions (ALS and ULS) due to the reduced canopy occlusion effect (Bauwens et al., 2016, Cabo et al., 2018, Kuželka et al., 2022; Oveland et al., 2018).

Conversely, the difference in falsely detected trees among the scanning trajectories might have been caused by a difference in acquisition point densities among the two mapping approaches. In addition, most of

Table 4
Comparison of tree detection and DBH_E accuracy obtained from different scanning trajectories in relation to the overall 55 reference trees encountered in the field.

Scanning trajectory	Detected trees	Omission error	Commission error	TDR [%]	RMSE [cm]	RMSE [%]	Bias [cm]	Bias [%]
Scan A	55	0	7	100	2.43	10.73	0.44	1.96
Scan B	55	0	1	100	3.25	14.34	−0.2	−0.88

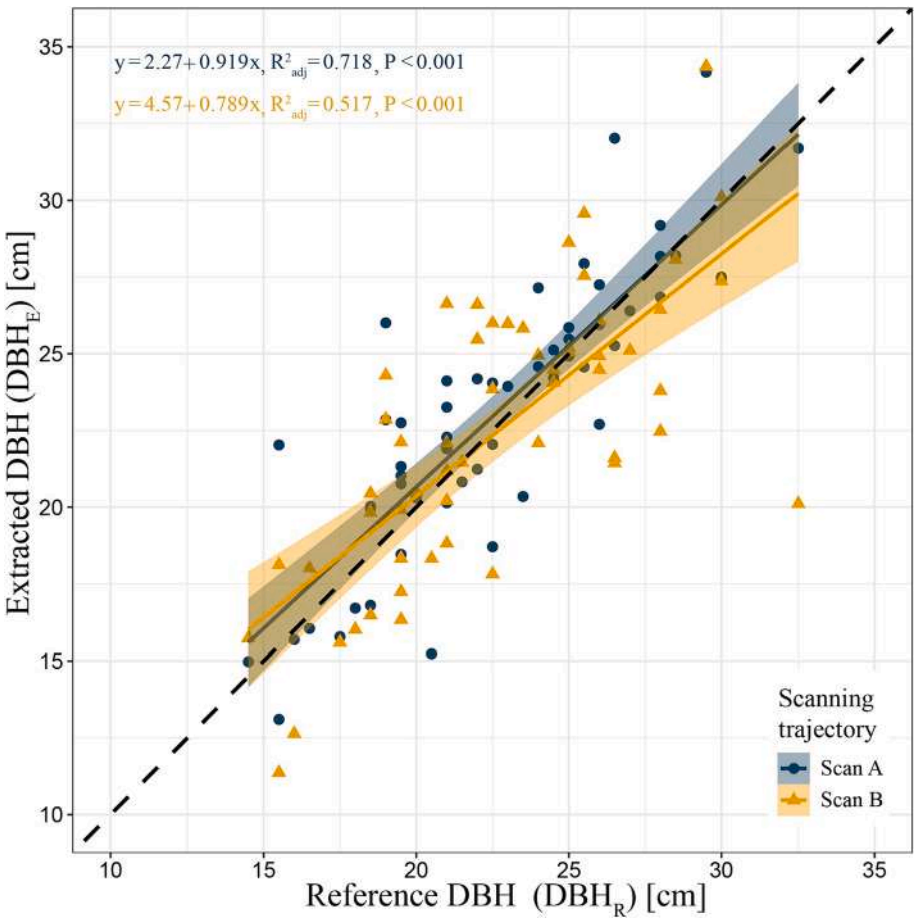

Fig. 6. Scatterplot of DBH_R versus DBH_E values and regression analyses. Points and fitted lines are coloured according to the scanning trajectory. Shaded colours show the 0.95 confidence region of the regression analyses. The dashed black line shows the 1:1 trend line for reference. The regression equations, proportions of the adjusted variance of DBH_E explained by DBH_R (R^2_{adj}) and statistical significances (P) are shown.

Table 5
Comparison of efficiency among traditional and RMLS survey methods.

Survey method	Personnel	Scanning trajectory	Survey task	Time taken [min:sec]	Surface monitored [m^2/min]	Trees monitored [trees/min]
Traditional	2		Plot placement	37:42	3.45	0.32
			DBH_R measurement	49:18		
			Overall	87:00		
RMLS	2	A	Point cloud acquisition	12:32	19.31	1.77
			Point cloud processing and DBH_E measurement	3:00		
			Overall	15:32		
		B	Point cloud acquisition	18:31	13.94	1.28
			Point cloud processing and DBH_E measurement	3:00		
			Overall	21:31		

falsely detected trees are located in plot 1 (five out of seven). It is then possible that a higher presence of tree lateral branches and/or shrubs in this zone were more intensively detected by scan A, creating a local higher amount of falsely detected trees. It is also worth mentioning that the amount of falsely detected trees is closely related to the noise levels of the point cloud and the influence of tree branches and understory vegetation. Point cloud filtering is then a crucial step of point cloud data pre-processing. However, methods for point cloud filtering and setting threshold limits are often based on empirical evaluations and vary in literature according to visual inspection of the point cloud (Kuželka et al., 2022). In our study, we applied the same point cloud filtering method for all plots and scanning trajectories. This filtering standardisation might have caused the difference in falsely detected trees among scanning trajectories.

Our study demonstrated that structural data collection using our RMLS survey protocol in beech forest of habitat 9110 provides satisfactory DBH_E values, with a RMSE of 10.73 % (2.43 cm) using circular scan trajectories. These values are in line with general requirements for DBH accuracy, which are approximately 2 cm (Liang et al., 2016). Also, our results on DBH_E using a quadrupedal robot to carry out a RMLS survey are in line with other studies that evaluate SLAM-based MLS accuracy in forest inventories, demonstrating a better performance of

LiDAR technologies instead of traditional calliper measurements (Giannetti et al., 2018; Spadavecchia et al., 2022). Early studies involving backpack-mounted MLS surveys reached DBH RMSE values higher than 12 % (Liang et al., 2014). More recent works usually equip handheld MLS such as Zeb-Revo lidar by Geoslam company, assessing DBH accuracies that are ranging from 0.8 to 2.46 cm (less than 10 %: Vatandaşlar and Zeybek, 2021; 10.8 %: Chiappini et al., 2022; 12.01 %: Gollob et al., 2020). In comparison, previous DBH acquisition protocols applied using a teleoperated legged robot in a European mixed fir and beech forest reached RMSE values between 16.9 cm (39.6 %) and 24.3 cm (56.9 %), achieving the identification of 37.78 to 97.77 % trees with a DBH >20 cm (Chirici et al., 2023).

Furthermore, our results also showed, even though both scanning trajectories successfully represented the plot in terms of TDR, that exist a difference in DBH_E accuracy among the scanning trajectories, featuring a better result of 10.73 % RMSE in circular trajectory (scan A) compared to 14.34 % RMSE in star-shaped trajectory (scan B). This result is partially contrasting with previous works on the argument (Kuželka et al., 2022). In their work, Kuželka et al. (2022) compared three different trajectories in forest handheld MLS point cloud acquisition and found that star-shaped trajectories were the most stable in terms of efficiency and point density uniformity. However, as these authors confirmed, the point density of a MLS acquisition depends on several factors that influence the speed of point cloud acquisition. A different localised speed of our legged robot due to obstruction of lying dead wood might then explain the difference in accuracy among the scanning trajectories. In fact, several studies warn on excessively dense acquisitions, which may cause drifts within the point cloud (Mokroš et al., 2021) or increase the number of outliers and the representation of twigs, lateral branches, leaves and shrubs in the point cloud (Chen et al., 2019). Finally, as also pointed out by the study of Kükenbrink et al. (2022), our choice to analyse all plots for both scanning trajectory types using the same filtering parameters might have negatively influenced the amount of falsely detected trees and DBH_E accuracy. Structural complexity, understory occlusion and the consequent number of outliers may have in fact varied among each plot and each scanning trajectory. Hence, we advocate that the application of RMLS surveys in EU forest structural habitat monitoring should take in consideration a plot-based point cloud processing to optimise results. Moreover, our results suggest that different DBH_E accuracies and falsely detected trees in RMLS point cloud acquisitions are trajectory-dependent.

The simpler circular trajectory of scan A was less difficult to perform and more efficient than scan B. However, even by moving on a longer trajectory, scan B was four times more efficient than a traditional structural survey. It is worth noting that the structural monitoring of forest habitats was not previously assessed with the use of a legged robot, hence there is a lack of information on the comparison between the efficiency of RMSL and traditional surveys. Moreover, previous studies that compared the efficiency of human-carried MLS in forest inventories with traditional survey methods measured different survey tasks, survey areas and stem densities, furtherly reducing the comparability of the survey efficiency among methods. For example, Ryding et al. (2015) used a handheld MLS (ZEB1) to measure DBH in semi-natural deciduous woodlands with a variable stem density ranging from 0.27 to 0.79 stems/m^2. They measured only time spent for field data acquisition and found that a surveyor equipped with handheld MLS was able to acquire the point cloud of a 100 m^2 plot in 20 m^2/min. In comparison, four people surveyed 2500 m^2 using traditional survey methods, achieving a surface coverage per surveyor of 0.43 m^2/min. Conversely, Ko et al. (2021) used a backpack-mounted MLS (Libackpack D50) in a wood plantation with an average stem density of 0.39 stems/m^2. They compared both fieldwork and office work among methods, measuring DBH and height of trees. They found that the handheld MLS survey was carried out at a surface coverage per surveyor of 20.2 to 25.5 m^2/min compared to 4.7 to 7.9 m^2/min of the traditional survey. It is possible then to speculate that the stem density of the surveyed area, its total surface and the different measurement operations have a higher influence on traditional survey time compared to the MLS survey. Hence, to better interpret the efficiency of structural survey methods, we advocate to standardise the measurement of survey efficiency on the basis of the number of measured trees per minute and differentiate the survey time according to single measurement operations (tree DBH, height, etc.) and single survey tasks (DBH_R measurement, point cloud acquisition, point cloud processing, etc.). In future, with the advancement of RMLS surveys, field measurements will be carried out by a single surveyor equipped with a legged robot able to autonomously carry out the structural survey (Pollayil et al., 2023). This will further enhance the efficiency of the RMLS structural survey by twofold compared to our results.

Future works should better focus on robot energetic efficiency and accuracy of extracted structural parameters based on point cloud processing parameters. For instance, employing autonomous locomotion and implementing terrain-aware locomotion algorithms could enable the robot to autonomously choose the most energetically efficient path to scan the plot depending on the specific ground and terrain conditions. Moreover, exploring the variation in different forest settings can provide valuable insights into the applicability and adaptability of RMLS-based surveys in structural EU habitat monitoring. Finally, the workflow and the derived processing script implemented by this research can be used as a reference to perform habitat monitoring assessments of CS using robotic assistance to extract structural data in similar forest habitats.

Future developments of this research could include the study of the effectiveness of RMLS in different forest habitats with diverse overstory and understory composition and structure. Additionally, it can be possible to consider measuring other important structural parameters such as tree height. Incorporating the measurement of tree height can enhance the capability of the method to assess the forest vertical structure, providing a more detailed perspective on the forest three-dimensional arrangement. With a wider adoption of RMLS surveys, future works will focus on efficiency and accuracy comparisons with HMLS surveys. Also, a combination of RMLS and ULS data acquisition modalities and multi-year measures to detect changes over time (e.g. Spadavecchia et al., 2022) will be developed. In fact, efficient above and below tree canopy data will be of use to capture a more complete vision of forest habitats (Ehrlich-Sommer et al., 2024). These approaches may also uncover unique patterns and dynamics in different EU forest habitats, contributing to a more robust habitat CS monitoring.

CRediT authorship contribution statement

Leopoldo de Simone: Writing – original draft, Visualization, Validation, Software, Resources, Methodology, Investigation, Formal analysis, Data curation, Conceptualization. **Emanuele Fanfarillo:** Writing – review & editing, Methodology, Investigation, Funding acquisition, Conceptualization. **Simona Maccherini:** Writing – review & editing, Validation, Supervision, Resources, Methodology, Funding acquisition. **Tiberio Fiaschi:** Writing – review & editing, Investigation. **Giuseppe Alfonso:** Writing – review & editing, Resources, Investigation. **Franco Angelini:** Writing – review & editing, Resources, Methodology, Investigation, Conceptualization. **Manolo Garabini:** Writing – review & editing, Supervision, Resources, Project administration, Investigation, Funding acquisition. **Claudia Angiolini:** Writing – review & editing, Writing – original draft, Supervision, Project administration, Methodology, Investigation, Conceptualization.

Declaration of competing interest

The authors declare that they have no known competing financial interests or personal relationships that could have appeared to influence the work reported in this paper.

Data availability

The data are available in Supplementary material

Acknowledgments

Field support was given by the group Carabinieri Biodiversity Department Vallombrosa. This research is partially supported by the European Union's Horizon 2020 Research and Innovation Programme under Grant Agreement No. 101016970 (Natural Intelligence), in part by the Ministry of University and Research (MUR) as part of the PON 2014-2021 "Research and Innovation" resources – Green/Innovation Action – DM MUR 1062/2021, and in part by the Italian Ministry of Education and Research (MIUR) in the framework of the FoReLab project (Departments of Excellence). E. Fanfarillo, S. Maccherini, and C. Angiolini were funded under the National Recovery and Resilience Plan (NRRP), Mission 4 Component 2 Investment 1.4 - Call for tender No. 3138 of 16 December 2021, rectified by Decree n.3175 of 18 December 2021 of Italian Ministry of University and Research funded by the European Union – NextGenerationEU; Award Number: Project code CN_00000033, Concession Decree No. 1034 of 17 June 2022 adopted by the Italian Ministry of University and Research, CUP B63C22000650007, Project title "National Biodiversity Future Center - NBFC".

Appendix A. Supplementary data

Supplementary data to this article can be found online at https://doi.org/10.1016/j.ecolind.2024.111882.

References

Alberdi, I., Nunes, L., Kovac, M., Bonheme, I., Cañellas, I., Rego, F.C., Gasparini, P., 2019. The conservation status assessment of natura 2000 forest habitats in Europe: capabilities, potentials and challenges of national forest inventories data. Annals of Forest Science 76 (2), 1–15. https://doi.org/10.1007/s13595-019-0820-4.

Angelini P., Casella L., Grignetti A., Genovesi P. (ed.) (2016). Manuali per il monitoraggio di specie e habitat di interesse comunitario (Direttiva 92/43/CEE) in Italia: habitat. ISPRA, Serie Manuali e linee guida, 142/2016.

Angelini, F., Angelini, P., Angiolini, C., Bagella, S., Bonomo, F., Caccianiga, M., ... & Garabini, M., 2023a. Robotic Monitoring of Habitats: The Natural Intelligence Approach. IEEE Access, vol. 11, pp. 72575-72591. 10.1109/ACCESS.2023.3294276.

Angelini, F., Pollayil, M.J., Bonini, F., Gigante, D., Garabini, M., 2023b. Robotic monitoring of grasslands: a dataset from the EU natura 2000 habitat 6210* in the central apennines (Italy). Scientific Data 10 (1), 418. https://doi.org/10.1038/s41597-023-02312-x.

Angelini, F., Pollayil, M., Valle, B., Borgatti, M.S., Caccianiga, M., Garabini, M., 2023c. Robotic monitoring of Alpine screes: a dataset from the EU natura 2000 habitat 8110 in the italian Alps. Sci Data 10, 855. https://doi.org/10.1038/s41597-023-02764-1.

Angelini, F., Pollayil, M.J., Rivieccio, G., Caria, M.C., Bagella, S., Garabini, M., 2024. Robotic monitoring of dunes: a dataset from the EU habitats 2110 and 2120 in Sardinia (Italy). Scientific Data 11 (1), 238. https://doi.org/10.1038/s41597-024-03063-z.

Angiolini, C., Foggi, B., Sarmati, S., Gabellini, A., Gennai, M., Castagnini, P., Mugnai, M., Viciani, D., Fanfarillo, E., Maccherini, S., 2021. Assessing the conservation status of EU forest habitats: The case of Quercus suber woodlands. For. Ecol. Manage. 496, 119432 https://doi.org/10.1016/j.foreco.2021.119432.

Anybotics, 2022. https://www.anybotics.com/anymal-specifications-sheet/(Accessed 20 October 2023).

Baker, R.L., Pearson, H.A., 1981. Plot delineation with a pin-and-chain. Jour. Range Mgmt. 34, 336–337.

Balenović, I., Liang, X., Jurjević, L., Hyyppä, J., Seletković, A., Kukko, A., 2021. Hand-held personal laser scanning–current status and perspectives for forest inventory application. Croatian Journal of Forest Engineering: Journal for Theory and Application of Forestry Engineering 42 (1), 165–183. https://doi.org/10.5552/crojfe.2021.858.

Barbati, A., Marchetti, M., Chirici, G., Corona, P., 2014. European Forest types and Forest Europe SFM indicators: tools for monitoring progress on forest biodiversity conservation. For. Ecol. Manage. 321, 145–157. https://doi.org/10.1016/j.foreco.2013.07.004.

Bauwens, S., Bartholomeus, H., Calders, K., Lejeune, P., 2016. Forest inventory with terrestrial LiDAR: a comparison of static and hand-held mobile laser scanning. Forests 7 (6), 127. https://doi.org/10.3390/f7060127.

Beers, T.W., 1962. Components of Forest Growth. J. for 60 (4), 245–248.

Brede, B., Lau, A., Bartholomeus, H.M., Kooistra, L., 2017. Comparing RIEGL RiCOPTER UAV LiDAR derived canopy height and DBH with terrestrial LiDAR. Sensors 17 (10), 2371. https://doi.org/10.3390/s17102371.

Brede, B., Calders, K., Lau, A., Raumonen, P., Bartholomeus, H.M., Herold, M., Kooistra, L., 2019. Non-destructive tree volume estimation through quantitative structure modelling: Comparing UAV laser scanning with terrestrial LIDAR. Remote Sensing of Environment 233, 111355. https://doi.org/10.1016/j.rse.2019.111355.

Brede, B., Bartholomeus, H.M., Barbier, N., Pimont, F., Vincent, G., Herold, M., 2022. Peering through the thicket: effects of UAV LiDAR scanner settings and flight planning on canopy volume discovery. International Journal of Applied Earth Observation and Geoinformation 114, 103056. https://doi.org/10.1016/j.jag.2022.103056.

Brown, J. K., 1974. Handbook for inventorying clowned woody material. U.S.D.A. Forest Service General Technical Report INT-16. Intermountain Forest & Range Experiment Station, Ogclen, UT. 24 pp.

Buchelt, A., Adrowitzer, A., Kieseberg, P., Gollob, C., Nothdurft, A., Eresheim, S., Tschiatschek, S., Stampfer, K., Holzinger, A., Holzinger, A., 2024. Exploring artificial intelligence for applications of drones in forest ecology and management. Forest Ecology and Management 551, 121530. https://doi.org/10.1016/j.foreco.2023.121530.

Bunce, R. G. H., Bogers, M.M.B., Roche, P., Walczak, M., Geijzendorffer, I.R., & Jongman. R.H.G., 2011. Manual for habitat and vegetation surveillance and monitoring: temperate, mediterranean and desert biomes. Tech. Rep., Alterra. ISSN 1566-7197.

Cabo, C., Del Pozo, S., Rodríguez-Gonzálvez, P., Ordóñez, C., González-Aguilera, D., 2018. Comparing terrestrial laser scanning (TLS) and wearable laser scanning (WLS) for individual tree modeling at plot level. Remote Sensing 10 (4), 540. https://doi.org/10.3390/rs10040540.

Čerňava, J., Tuček, J., Koreň, M., Mokroš, M., 2017. Estimation of diameter at breast height from mobile laser scanning data collected under a heavy forest canopy. Journal of Forest Science 63 (9), 433–441. https://doi.org/10.17221/28/2017-JFS.

Chang, A., Jung, J., Kim, Y., 2015. Estimation of forest stand diameter class using airborne lidar and field data. Remote Sensing Letters 6 (6), 419–428. https://doi.org/10.1080/2150704X.2015.1035770.

Chen, S., Liu, H., Feng, Z., Shen, C., Chen, P., 2019. Applicability of personal laser scanning in forestry inventory. PLoS One 14 (2), e0211392.

Chiappini, S., Pierdicca, R., Malandra, F., Tonelli, E., Malinverni, E.S., Urbinati, C., Vitali, A., 2022. Comparing Mobile laser scanner and manual measurements for dendrometric variables estimation in a black pine (Pinus nigra arn.) plantation. Computers and Electronics in Agriculture 198, 107069. https://doi.org/10.1016/j.compag.2022.107069.

Chirici, G., McRoberts, R.E., Winter, S., Bertini, R., Brändli, U.B., Asensio, I.A., Marchetti, M., 2012. National forest inventory contributions to forest biodiversity monitoring. Forest Science 58 (3), 257–268. https://doi.org/10.5849/forsci.12-003.

Chirici, G., Giannetti, F., D'Amico, G., Vangi, E., Francini, S., Borghi, C., Travaglini, D., 2023. Robotics in Forest inventories: SPOT's first steps. Forests 14 (11), 2170. https://doi.org/10.3390/f14112170.

Chytrý, M., Otýpková, Z., 2003. Plot sizes used for phytosociological sampling of european vegetation. Journal of Vegetation Science 14 (4), 563–570. https://doi.org/10.1111/j.1654-1103.2003.tb02183.x.

Chytrý, M., Tichý, L., Hennekens, S.M., Knollová, I., Janssen, J.A., Rodwell, J.S., Schaminée, J.H., 2020. EUNIS habitat classification: expert system, characteristic species combinations and distribution maps of european habitats. Applied Vegetation Science 23 (4), 648–675. https://doi.org/10.1111/avsc.12519.

CloudCompare (version 2.12) [GPL software]., 2023. Retrieved from http://www.cloudcompare.org/.

Corona, P., Chirici, G., McRoberts, R.E., Winter, S., Barbati, A., 2011. Contribution of large-scale forest inventories to biodiversity assessment and monitoring. Forest Ecology and Management 262 (11), 2061–2069. https://doi.org/10.1016/j.foreco.2011.08.044.

Curtis, R.O.; Marshall, D.D., 2005. Permanent-plot procedures for silvicultural and yield research. Gen. Tech. Rep. PNW-GTR-634. Portland, OR: U.S. Department of Agriculture, Forest Service, Pacific Northwest Research Station. 86 p.

Dalla Corte, A.P., Rex, F.E., Almeida, D.R.A.D., Sanquetta, C.R., Silva, C.A., Moura, M.M., Broadbent, E.N., 2020. Measuring individual tree diameter and height using GatorEye high-density UAV-Lidar in an integrated crop-livestock-forest system. Remote Sensing 12 (5), 863. https://doi.org/10.3390/rs12050863.

de Conto, T., Olofsson, K., Görgens, E.B., Rodriguez, L.C.E., Almeida, G., 2017. Performance of stem denoising and stem modelling algorithms on single tree point clouds from terrestrial laser scanning. Computers and Electronics in Agriculture 143, 165–176. https://doi.org/10.1016/j.compag.2017.10.019.

Ehrlich-Sommer, F., Hoenigsberger, F., Gollob, C., Nothdurft, A., Stampfer, K., Holzinger, A., 2024. Sensors for digital transformation in Smart forestry. Sensors 24 (3), 798. https://doi.org/10.3390/s24030798.

Ellwanger, G., Runge, S., Wagner, M., Ackermann, W., Neukirchen, M., Frederking, W., Sukopp, U., 2018. Current status of habitat monitoring in the European Union according to article 17 of the habitats directive, with an emphasis on habitat structure and functions and on Germany. Nature Conservation 29, 57–78. https://doi.org/10.3897/natureconservation.29.27273.

European Commission, 1992. Council directive 92/43/EEC of 21 may 1992 on the conservation of natural habitats and of wild fauna and flora. Official journal L 206, 22/07/1992. P. 0007-0050. Off. J. Eur. Union 206, 7–50.

Evans, D., Arvela, M., 2011. Assessment and reporting under article 17 of the habitats directive. explanatory notes & guidelines for the period 2007–2012. European Commission, Brussels.

Giannetti, F., Puletti, N., Quatrini, V., Travaglini, D., Bottalico, F., Corona, P., Chirici, G., 2018. Integrating terrestrial and airborne laser scanning for the assessment of single-

tree attributes in Mediterranean forest stands. European Journal of Remote Sensing 51 (1), 795–807. https://doi.org/10.1080/22797254.2018.1482733.
Gigante, D., Attorre, F., Venanzoni, R., Acosta, A.T.R., Agrillo, E., Aleffi, M., Zitti, S., 2016. A methodological protocol for annex I habitats monitoring: the contribution of vegetation science. Plant Sociology 53 (2), 77–87. https://doi.org/10.7338/pls2016532/06.
Gollob, C., Ritter, T., Nothdurft, A., 2020. Forest inventory with long range and high-speed personal laser scanning (PLS) and simultaneous localization and mapping (SLAM) technology. Remote Sensing 12 (9), 1509. https://doi.org/10.3390/rs12091509.
Gollob, C., Krassnitzer, R., Ritter, T., Tockner, A., Erber, G., Kühmaier, M., Hönigsberger, F., Varch, T., Holzinger, A., Stampfer, K., Nothdurft, A., 2023. Measurement of individual tree Parameters with Carriage-based laser scanning in cable Yarding operations. Croatian Journal of Forest Engineering: Journal for Theory and Application of Forestry Engineering 44 (2), 401–417. https://doi.org/10.5552/crojfe.2023.2252.
Hackel, T., Wegner, J. D., & Schindler, K., 2016. Contour detection in unstructured 3D point clouds. In Proceedings of the IEEE conference on computer vision and pattern recognition (pp. 1610-1618).
Holopainen, M., Kankare, V., Vastaranta, M., Liang, X., Lin, Y., Vaaja, M., Alho, P., 2013. Tree mapping using airborne, terrestrial and mobile laser scanning–a case study in a heterogeneous urban forest. Urban Forestry & Urban Greening 12 (4), 546–553. https://doi.org/10.1016/j.ufug.2013.06.002.
Hutter, M., Gehring, C., Lauber, A., Gunther, F., Bellicoso, C.D., Tsounis, V., Meyer, K., 2017. Anymal-toward legged robots for harsh environments. Advanced Robotics 31 (17), 918–931. https://doi.org/10.1080/01691864.2017.1378591.
Hyyppä, J., Inkinen, M., 1999. Detecting and estimating attributes for single trees using laser scanner. Photogramm. J. Fin 16, 27–42.
Illingworth, J., Kittler, J., 1987. The adaptive hough transform. IEEE Transactions on Pattern Analysis and Machine Intelligence 5, 690–698. https://doi.org/10.1109/TPAMI.1987.4767964.
Kankare, V., Vauhkonen, J., Tanhuanpää, T., Holopainen, M., Vastaranta, M., Joensuu, M., Viitala, R., 2014. Accuracy in estimation of timber assortments and stem distribution–a comparison of airborne and terrestrial laser scanning techniques. ISPRS Journal of Photogrammetry and Remote Sensing 97, 89–97. https://doi.org/10.1016/j.isprsjprs.2014.08.008.
Kaur, P., Gigante, D., Caccianiga, M., Bagella, S., Angiolini, C., Garabini, M., Remagnino, P., 2023. In: Segmentation and Identification of Mediterranean Plant Species. Springer Nature Switzerland, Cham, pp. 431–442. https://doi.org/10.1007/978-3-031-47966-3_34.
Ko, C., Lee, S., Yim, J., Kim, D., Kang, J., 2021. Comparison of forest inventory methods at plot-level between a backpack personal laser scanning (bpls) and conventional equipment in jeju island, south korea. Forests 12 (3), 308. https://doi.org/10.3390/f12030308.
Köhl, M., Magnussen, S., Marchetti, M., 2006. Sampling Methods, Remote Sensing and GIS Multiresource Forest Inventory, 2. Springer, Berlin.
Kovač, M., Bauer, A., Ståhl, G., 2014. Merging national forest and national forest health inventories to obtain an integrated forest resource inventory–experiences from Bavaria. Slovenia and Sweden. Plos One 9 (6), e100157.
Krisanski, S., Del Perugia, B., Taskhiri, M. S., & Turner, P., 2018. Below-canopy UAS photogrammetry for stem measurement in radiata pine plantation. In Remote Sensing for Agriculture, Ecosystems, and Hydrology XX (Vol. 10783, pp. 45-55). SPIE. 10.1117/12.2325480.
Kükenbrink, D., Marty, M., Bösch, R., Ginzler, C., 2022. Benchmarking laser scanning and terrestrial photogrammetry to extract forest inventory parameters in a complex temperate forest. International Journal of Applied Earth Observation and Geoinformation 113, 102999. https://doi.org/10.1016/j.jag.2022.102999.
Kuuluvainen, T., 2009. Forest management and biodiversity conservation based on natural ecosystem dynamics in northern Europe: the complexity challenge. AMBIO: a journal of the human. Environment 38 (6), 309–315. https://doi.org/10.1579/08-A-490.1.
Kuželka, K., Marušák, R., Surový, P., 2022. Inventory of close-to-nature forest stands using terrestrial mobile laser scanning. International Journal of Applied Earth Observation and Geoinformation 115, 103104. https://doi.org/10.1016/j.jag.2022.103104.
Lee, J., Hwangbo, J., Hutter, M., 2019. Robust recovery controller for a quadrupedal robot using deep reinforcement learning. arXiv preprint arXiv:1901.07517.
Lee, J., Hwangbo, J., Wellhausen, L., Koltun, V., Hutter, M., 2020. Learning quadrupedal locomotion over challenging terrain. Science Robotics 5 (47), eabc5986. https://doi.org/10.1126/scirobotics.abc5986.
Liang, X., Kukko, A., Kaartinen, H., Hyyppä, J., Yu, X., Jaakkola, A., Wang, Y., 2014. Possibilities of a personal laser scanning system for forest mapping and ecosystem services. Sensors 14 (1), 1228–1248. https://doi.org/10.3390/s140101228.
Liang, X., Kankare, V., Hyyppä, J., Wang, Y., Kukko, A., Haggrén, H., Vastaranta, M., 2016. Terrestrial laser scanning in forest inventories. ISPRS Journal of Photogrammetry and Remote Sensing 115, 63–77. https://doi.org/10.1016/j.isprsjprs.2016.01.006.
Liang, X., Kukko, A., Hyyppä, J., Lehtomäki, M., Pyörälä, J., Yu, X., Wang, Y., 2018. In-situ measurements from mobile platforms: an emerging approach to address the old challenges associated with forest inventories. ISPRS Journal of Photogrammetry and Remote Sensing 143, 97–107. https://doi.org/10.1016/j.isprsjprs.2018.04.019.
Lindenmayer, D.B., Margules, C.R., Botkin, D.B., 2000. Indicators of biodiversity for ecologically sustainable forest management. Conservation Biology 14 (4), 941–950. https://doi.org/10.1046/j.1523-1739.2000.98533.x.
Liu, G., Wang, J., Dong, P., Chen, Y., Liu, Z., 2018. Estimating individual tree height and diameter at breast height (DBH) from terrestrial laser scanning (TLS) data at plot level. Forests 9 (7), 398. https://doi.org/10.3390/f9070398.
Manh, X. H., Gigante, D., Angiolini, C., Bagella, S., Caccianiga, M., Angelini, F., ... & Remagnino, P., 2022. Karlinsky, L., Michaeli, T., Nishino, K. (eds) Computer Vision – ECCV 2022 Workshops. ECCV 2022. Lecture Notes in Computer Science, vol 13806. Springer, Cham. 10.1007/978-3-031-25075-0_51.
Maas, H.G., Bienert, A., Scheller, S., Keane, E., 2008. Automatic forest inventory parameter determination from terrestrial laser scanner data. Int. J. Remote Sens. 29 (5), 1579–1593. https://doi.org/10.1080/01431160701736406.
Mokroš, M., Mikita, T., Singh, A., Tomaštík, J., Chudá, J., Wężyk, P., Liang, X., 2021. Novel low-cost mobile mapping systems for forest inventories as terrestrial laser scanning alternatives. International Journal of Applied Earth Observation and Geoinformation 104, 102512. https://doi.org/10.1016/j.jag.2021.102512.
Moran, L.A., Williams, R.A., 2002. Field note—Comparison of three dendrometers in measuring diameter at breast height field note. Northern Journal of Applied Forestry 19 (1), 28–33. https://doi.org/10.1093/njaf/19.1.28.
Oliveira, L.F., Moreira, A.P., Silva, M.F., 2021. Advances in forest robotics: a state-of-the-art survey. Robotics 10 (2), 53. https://doi.org/10.3390/robotics10020053.
Oveland, I., Hauglin, M., Giannetti, F., Schipper Kjørsvik, N., Gobakken, T., 2018. Comparing three different ground based laser scanning methods for tree stem detection. Remote Sens 10 (4), 538. https://doi.org/10.3390/rs10040538.
Paris, C., Kelbe, D., van Aardt, J., & Bruzzone, L., 2015. A precise estimation of the 3D structure of the forest based on the fusion of airborne and terrestrial LiDAR data. In 2015 IEEE International Geoscience and Remote Sensing Symposium (IGARSS) (pp. 49-52). IEEE. Doi:10.1109/IGARSS.2015.7325694.
Pierzchała, M., Giguère, P., Astrup, R., 2018. Mapping forests using an unmanned ground vehicle with 3D LiDAR and graph-SLAM. Computers and Electronics in Agriculture 145, 217–225. https://doi.org/10.1016/j.compag.2017.12.034.
Pollayil, M., Angelini, F., de Simone, L., Fanfarillo, E., Fiaschi, T., Maccherini, S., Angiolini, C., Garabini, M., 2023. Robotic monitoring of forests: a dataset from the EU habitat 9210* in the Tuscan Apennines (central Italy). Sci. Data 10, 845. https://doi.org/10.1038/s41597-023-02763-2.
R: A language and environment for statistical computing. R Foundation for Statistical Computing, Vienna, Austria. URL https://www.R-project.org/.
Raison, R. J., Flinn, D. W., & Brown, A. G., 2001. Application of criteria and indicators to support sustainable forest management: some key issues. In 'Criteria and indicators for sustainable forest management'. Papers presented at a IUFRO/CIFOR/FAO conference 'Sustainable forest management: fostering stakeholder input to advance development of scientifically based indicators', Melbourne, Australia 10.1079/9780851993928.0005.
Roussel, J.R., Auty, D., Coops, N.C., Tompalski, P., Goodbody, T.R., Meador, A.S., Achim, A., 2020. lidR: an R package for analysis of airborne laser scanning (ALS) data. Remote Sensing of Environment 251, 112061. https://doi.org/10.1016/j.rse.2020.112061.
Rusu, R.B., Cousins, S., 2011. 3d is here: point cloud library (pcl). In: In 2011 IEEE International Conference on Robotics and Automation. IEEE, pp. 1–4. https://doi.org/10.1109/ICRA.2011.5980567.
Ryding, J., Williams, E., Smith, M.J., Eichhorn, M.P., 2015. Assessing handheld mobile laser scanners for forest surveys. Remote Sensing 7 (1), 1095–1111. https://doi.org/10.3390/rs70101095.
Schneider, F.D., Kükenbrink, D., Schaepman, M.E., Schimel, D.S., Morsdorf, F., 2019. Quantifying 3D structure and occlusion in dense tropical and temperate forests using close-range LiDAR. Agricultural and Forest Meteorology 268, 249–257. https://doi.org/10.1016/j.agrformet.2019.01.033.
Simonse, M., Aschoff, T., Spiecker, H., & Thies, M., 2003. Automatic determination of forest inventory parameters using terrestrial laser scanning. In Proceedings of the scandlaser scientific workshop on airborne laser scanning of forests (Vol. 2003, pp. 252-258). Umeå: Sveriges Lantbruksuniversitet.
Sivanpillai, R., Brown, G.K., Gellis, B.S., 2019. In: Flying UAVS in Constrained Environments: Best Practices for Flying within Complex Forest Canopies. CRC Press, pp. 269–281.
Spadavecchia, C., Belcore, E., Piras, M., Kobal, M., 2022. An automatic individual tree 3D change detection method for allometric Parameters estimation in mixed uneven-aged Forest stands from ALS data. Remote Sensing 14 (18), 4666. https://doi.org/10.3390/rs14184666.
Srinivasan, S., Popescu, S.C., Eriksson, M., Sheridan, R.D., Ku, N.W., 2015. Terrestrial laser scanning as an effective tool to retrieve tree level height, crown width, and stem diameter. Remote Sensing 7 (2), 1877–1896. https://doi.org/10.3390/rs70201877.
Storch, F., Dormann, C.F., Bauhus, J., 2018. Quantifying forest structural diversity based on large-scale inventory data: a new approach to support biodiversity monitoring. Forest Ecosystems 5 (1), 1–14. https://doi.org/10.1186/s40663-018-0151-1.
Sun, L., Fang, L., Tang, L., Liu, J., 2018. Developing portable system for measuring diameter at breast height. Journal of Beijing Forestry University 40 (9), 82–89. https://doi.org/10.13332/j.1000-1522.20180102.
Terryn, L., Calders, K., Bartholomeus, H., Bartolo, R.E., Brede, B., D'hont, B., Verbeeck, H., 2022. Quantifying tropical forest structure through terrestrial and UAV laser scanning fusion in australian rainforests. Remote Sensing of Environment 271, 112912. https://doi.org/10.1016/j.rse.2022.112912.
Torres-Pardo, A., Pinto-Fernández, D., Garabini, M., Angelini, F., Rodriguez-Cianca, D., Massardi, S., Torricelli, D., 2022. Legged locomotion over irregular terrains: state of the art of human and robot performance. Bioinspiration & Biomimetics 17 (6), 061002. https://doi.org/10.1088/1748-3190/ac92b3.

Tremblay, J. F., Beland, M., Gagnon, R., Pomerleau, F., & Giguère, P., 2020. Automatic three-dimensional mapping for tree diameter measurements in inventory operations. Journal of Field Robotics 37(8), 1328-1346. 10.48550/arXiv.1904.05281.

Tuscany Region, 2022. La carta degli habitat nei siti Natura 2000 toscani. https://www.regione.toscana.it/-/la-carta-degli-habitat-nei-siti-natura-2000-toscani (Accessed 20 October 2022).

Vandendaele, B., Fournier, R.A., Vepakomma, U., Pelletier, G., Lejeune, P., Martin-Ducup, O., 2021. Estimation of northern hardwood forest inventory attributes using UAV laser scanning (ULS): transferability of laser scanning methods and comparison of automated approaches at the tree-and stand-level. Remote Sensing 13 (14), 2796. https://doi.org/10.3390/rs13142796.

Vastaranta, M., Melkas, T., Holopainen, M., Kaartinen, H., Hyyppä, J., Hyyppä, H., 2009. Laser-based field measurements in tree-level forest data acquisition. Photogramm. J. Finl 21, 51–61.

Vatandaşlar, C., Zeybek, M., 2021. Extraction of forest inventory parameters using handheld mobile laser scanning: a case study from Trabzon. Turkey. Measurement 177, 109328. https://doi.org/10.1016/j.measurement.2021.109328.

Vauhkonen, J., Maltamo, M., McRoberts, R.E., Næsset, E., 2014. Introduction to forestry applications of airborne laser scanning. Forestry Applications of Airborne Laser Scanning: Concepts and Case Studies 1–16.

Vítková, L., Ní Dhubháin, Á., Pommerening, A., 2016. Agreement in tree marking: what is the uncertainty of human tree selection in selective forest management? Forest Science 62 (3), 288–296. https://doi.org/10.5849/forsci.15-133.

West, P.W., 2015. Tree and Forest. Measurement. https://doi.org/10.1007/978-3-319-14708-6.

Wilkes, P., Lau, A., Disney, M., Calders, K., Burt, A., de Tanago, J.G., Herold, M., 2017. Data acquisition considerations for terrestrial laser scanning of forest plots. Remote Sensing of Environment 196, 140–153. https://doi.org/10.1016/j.rse.2017.04.030.

Yang, C., Pu, C., Xin, G., Zhang, J., Li, Z., 2023. Learning complex motor skills for legged robot fall recovery. IEEE Robotics and Automation Letters. https://doi.org/10.1109/LRA.2023.3281290.

Zhang, Z., 1994. Iterative point matching for registration of free-form curves and surfaces. International Journal of Computer Vision 13 (2), 119–152. https://doi.org/10.1007/BF01427149.

Zhang, W., Qi, J., Wan, P., Wang, H., Xie, D., Wang, X., Yan, G., 2016. An easy-to-use airborne LiDAR data filtering method based on cloth simulation. Remote Sensing 8 (6), 501. https://doi.org/10.3390/rs8060501.